PHYSICAL REVIEW LETTERS **130,** 211901 (2023)

Precision Measurement of the Decay $\Sigma^+ \to p\gamma$ in the Process $J/\psi \to \Sigma^+\bar{\Sigma}^-$

M. Ablikim,[1] M. N. Achasov,[13,b] P. Adlarson,[73] R. Aliberti,[34] A. Amoroso,[72a,72c] M. R. An,[38] Q. An,[69,56] Y. Bai,[55] O. Bakina,[35] I. Balossino,[29a] Y. Ban,[45,g] V. Batozskaya,[1,43] K. Begzsuren,[31] N. Berger,[34] M. Bertani,[28a] D. Bettoni,[29a] F. Bianchi,[72a,72c] E. Bianco,[72a,72c] J. Bloms,[66] A. Bortone,[72a,72c] I. Boyko,[35] R. A. Briere,[5] A. Brueggemann,[66] H. Cai,[74] X. Cai,[1,56] A. Calcaterra,[28a] G. F. Cao,[1,61] N. Cao,[1,61] S. A. Cetin,[60a] J. F. Chang,[1,56] T. T. Chang,[75] W. L. Chang,[1,61] G. R. Che,[42] G. Chelkov,[35,a] C. Chen,[42] Chao Chen,[53] G. Chen,[1] H. S. Chen,[1,61] M. L. Chen,[1,56,61] S. J. Chen,[41] S. M. Chen,[59] T. Chen,[1,61] X. R. Chen,[30,61] X. T. Chen,[1,61] Y. B. Chen,[1,56] Y. Q. Chen,[33] Z. J. Chen,[25,h] W. S. Cheng,[72c] S. K. Choi,[10] X. Chu,[42] G. Cibinetto,[29a] S. C. Coen,[4] F. Cossio,[72c] J. J. Cui,[48] H. L. Dai,[1,56] J. P. Dai,[77] A. Dbeyssi,[19] R. E. de Boer,[4] D. Dedovich,[35] Z. Y. Deng,[1] A. Denig,[34] I. Denysenko,[35] M. Destefanis,[72a,72c] F. De Mori,[72a,72c] B. Ding,[64,1] X. X. Ding,[45,g] Y. Ding,[39] Y. Ding,[33] J. Dong,[1,56] L. Y. Dong,[1,61] M. Y. Dong,[1,56,61] X. Dong,[74] S. X. Du,[79] Z. H. Duan,[41] P. Egorov,[35,a] Y. L. Fan,[74] J. Fang,[1,56] S. S. Fang,[1,61] W. X. Fang,[1] Y. Fang,[1] R. Farinelli,[29a] L. Fava,[72b,72c] F. Feldbauer,[4] G. Felici,[28a] C. Q. Feng,[69,56] J. H. Feng,[57] K. Fischer,[67] M. Fritsch,[4] C. Fritzsch,[66] C. D. Fu,[1] Y. W. Fu,[1] H. Gao,[61] Y. N. Gao,[45,g] Yang Gao,[69,56] S. Garbolino,[72c] I. Garzia,[29a,29b] P. T. Ge,[74] Z. W. Ge,[41] C. Geng,[57] E. M. Gersabeck,[65] A. Gilman,[67] K. Goetzen,[14] L. Gong,[39] W. X. Gong,[1,56] W. Gradl,[34] S. Gramigna,[29a,29b] M. Greco,[72a,72c] M. H. Gu,[1,56] Y. T. Gu,[16] C. Y. Guan,[1,61] Z. L. Guan,[22] A. Q. Guo,[30,61] L. B. Guo,[40] R. P. Guo,[47] Y. P. Guo,[12,f] A. Guskov,[35,a] X. T. H.,[1,61] W. Y. Han,[38] X. Q. Hao,[20] F. A. Harris,[63] K. K. He,[53] K. L. He,[1,61] F. H. Heinsius,[4] C. H. Heinz,[34] Y. K. Heng,[1,56,61] C. Herold,[58] T. Holtmann,[4] P. C. Hong,[12,f] G. Y. Hou,[1,61] Y. R. Hou,[61] Z. L. Hou,[1] H. M. Hu,[1,61] J. F. Hu,[54,i] T. Hu,[1,56,61] Y. Hu,[1] G. S. Huang,[69,56] K. X. Huang,[57] L. Q. Huang,[30,61] X. T. Huang,[48] Y. P. Huang,[1] T. Hussain,[71] N. Hüsken,[27,34] W. Imoehl,[27] M. Irshad,[69,56] J. Jackson,[27] S. Jaeger,[4] S. Janchiv,[31] J. H. Jeong,[10] Q. Ji,[1] Q. P. Ji,[20] X. B. Ji,[1,61] X. L. Ji,[1,56] Y. Y. Ji,[48] Z. K. Jia,[69,56] P. C. Jiang,[45,g] S. S. Jiang,[38] T. J. Jiang,[17] X. S. Jiang,[1,56,61] Y. Jiang,[61] J. B. Jiao,[48] Z. Jiao,[23] S. Jin,[41] Y. Jin,[64] M. Q. Jing,[1,61] T. Johansson,[73] X. K.,[1] S. Kabana,[32] N. Kalantar-Nayestanaki,[62] X. L. Kang,[9] X. S. Kang,[39] R. Kappert,[62] M. Kavatsyuk,[62] B. C. Ke,[79] A. Khoukaz,[66] R. Kiuchi,[1] R. Kliemt,[14] L. Koch,[36] O. B. Kolcu,[60a] B. Kopf,[4] M. Kuessner,[4] A. Kupsc,[43,73] W. Kühn,[36] J. J. Lane,[65] J. S. Lange,[36] P. Larin,[19] A. Lavania,[26] L. Lavezzi,[72a,72c] T. T. Lei,[69,k] Z. H. Lei,[69,56] H. Leithoff,[34] M. Lellmann,[34] T. Lenz,[34] C. Li,[42] C. Li,[46] C. H. Li,[38] Cheng Li,[69,56] D. M. Li,[79] F. Li,[1,56] G. Li,[1] H. Li,[69,56] H. B. Li,[1,61] H. J. Li,[20] H. N. Li,[54,i] Hui Li,[42] J. R. Li,[59] J. S. Li,[57] J. W. Li,[48] Ke Li,[1] L. J. Li,[1,61] L. K. Li,[1] Lei Li,[3] M. H. Li,[42] P. R. Li,[37,j,k] S. X. Li,[12] T. Li,[48] W. D. Li,[1,61] W. G. Li,[1] X. H. Li,[69,56] X. L. Li,[48] Xiaoyu Li,[1,61] Y. G. Li,[45,g] Z. J. Li,[57] Z. X. Li,[16] Z. Y. Li,[57] C. Liang,[41] H. Liang,[69,56] H. Liang,[1,61] H. Liang,[33] Y. F. Liang,[52] Y. T. Liang,[30,61] G. R. Liao,[15] L. Z. Liao,[48] J. Libby,[26] A. Limphirat,[58] D. X. Lin,[30,61] T. Lin,[1] B. J. Liu,[1] B. X. Liu,[74] C. Liu,[33] C. X. Liu,[1] D. Liu,[19,69] F. H. Liu,[51] Fang Liu,[1] Feng Liu,[6] G. M. Liu,[54,i] H. Liu,[37,j,k] H. B. Liu,[16] H. M. Liu,[1,61] Huanhuan Liu,[1] Huihui Liu,[21] J. B. Liu,[69,56] J. L. Liu,[70] J. Y. Liu,[1,61] K. Liu,[1] K. Y. Liu,[39] Ke Liu,[22] L. Liu,[69,56] L. C. Liu,[42] Lu Liu,[42] M. H. Liu,[12,f] P. L. Liu,[1] Q. Liu,[61] S. B. Liu,[69,56] T. Liu,[12,f] W. K. Liu,[42] W. M. Liu,[69,56] X. Liu,[37,j,k] Y. Liu,[37,j,k] Y. B. Liu,[42] Z. A. Liu,[1,56,61] Z. Q. Liu,[48] X. C. Lou,[1,56,61] F. X. Lu,[57] H. J. Lu,[23] J. G. Lu,[1,56] X. L. Lu,[1] Y. Lu,[7] Y. P. Lu,[1,56] Z. H. Lu,[1,61] C. L. Luo,[40] M. X. Luo,[78] T. Luo,[12,f] X. L. Luo,[1,56] X. R. Lyu,[61] Y. F. Lyu,[42] F. C. Ma,[39] H. L. Ma,[1] J. L. Ma,[1,61] L. L. Ma,[48] M. M. Ma,[1,61] Q. M. Ma,[1] R. Q. Ma,[1,61] R. T. Ma,[61] X. Y. Ma,[1,56] Y. Ma,[45,g] F. E. Maas,[19] M. Maggiora,[72a,72c] S. Maldaner,[4] S. Malde,[67] A. Mangoni,[28b] Y. J. Mao,[45,g] Z. P. Mao,[1] S. Marcello,[72a,72c] Z. X. Meng,[64] J. G. Messchendorp,[14,62] G. Mezzadri,[29a] H. Miao,[1,61] T. J. Min,[41] R. E. Mitchell,[27] X. H. Mo,[1,56,61] N. Yu. Muchnoi,[13,b] Y. Nefedov,[35] F. Nerling,[19,d] I. B. Nikolaev,[13,b] Z. Ning,[1,56] S. Nisar,[11,l] Y. Niu,[48] S. L. Olsen,[61] Q. Ouyang,[1,56,61] S. Pacetti,[28b,28c] X. Pan,[53] Y. Pan,[55] A. Pathak,[33] Y. P. Pei,[69,56] M. Pelizaeus,[4] H. P. Peng,[69,56] K. Peters,[14,d] J. L. Ping,[40] R. G. Ping,[1,61] S. Plura,[34] S. Pogodin,[35] V. Prasad,[32] F. Z. Qi,[1] H. Qi,[69,56] H. R. Qi,[59] M. Qi,[41] T. Y. Qi,[12,f] S. Qian,[1,56] W. B. Qian,[61] C. F. Qiao,[61] J. J. Qin,[70] L. Q. Qin,[15] X. P. Qin,[12,f] X. S. Qin,[48] Z. H. Qin,[1,56] J. F. Qiu,[1] S. Q. Qu,[59] C. F. Redmer,[34] K. J. Ren,[38] A. Rivetti,[72c] V. Rodin,[62] M. Rolo,[72c] G. Rong,[1,61] Ch. Rosner,[19] S. N. Ruan,[42] N. Salone,[43] A. Sarantsev,[35,c] Y. Schelhaas,[34] K. Schoenning,[73] M. Scodeggio,[29a,29b] K. Y. Shan,[12,f] W. Shan,[24] X. Y. Shan,[69,56] J. F. Shangguan,[53] L. G. Shao,[1,61] M. Shao,[69,56] C. P. Shen,[12,f] H. F. Shen,[1,61] W. H. Shen,[61] X. Y. Shen,[1,61] B. A. Shi,[61] H. C. Shi,[69,56] J. Y. Shi,[1] Q. Q. Shi,[53] R. S. Shi,[1,61] X. Shi,[1,56] J. J. Song,[20] T. Z. Song,[57] W. M. Song,[33,1] Y. X. Song,[45,g] S. Sosio,[72a,72c] S. Spataro,[72a,72c] F. Stieler,[34] Y. J. Su,[61] G. B. Sun,[74] G. X. Sun,[1] H. Sun,[61] H. K. Sun,[1] J. F. Sun,[20] K. Sun,[59] L. Sun,[74] S. S. Sun,[1,61] T. Sun,[1,61] W. Y. Sun,[33] Y. Sun,[9] Y. J. Sun,[69,56] Y. Z. Sun,[1] Z. T. Sun,[48] Y. X. Tan,[69,56] C. J. Tang,[52] G. Y. Tang,[1] J. Tang,[57] Y. A. Tang,[74] L. Y. Tao,[70] Q. T. Tao,[25,h] M. Tat,[67] J. X. Teng,[69,56] V. Thoren,[73] W. H. Tian,[50] W. H. Tian,[57] Y. Tian,[30,61] Z. F. Tian,[74] I. Uman,[60b] B. Wang,[1] B. L. Wang,[61] Bo Wang,[69,56] C. W. Wang,[41] D. Y. Wang,[45,g] F. Wang,[70] H. J. Wang,[37,j,k] H. P. Wang,[1,61] K. Wang,[1,56] L. L. Wang,[1] M. Wang,[48] Meng Wang,[1,61] S. Wang,[37,j,k] S. Wang,[12,f] T. Wang,[12,f] T. J. Wang,[42]

0031-9007/23/130(21)/211901(9)

Published by the American Physical Society

W. Wang,[70] W. Wang,[57] W. H. Wang,[74] W. P. Wang,[69,56] X. Wang,[45,g] X. F. Wang,[37,j,k] X. J. Wang,[38] X. L. Wang,[12,f] Y. Wang,[59] Y. D. Wang,[44] Y. F. Wang,[1,56,61] Y. H. Wang,[46] Y. N. Wang,[44] Y. Q. Wang,[1] Yaqian Wang,[18,1] Yi Wang,[59] Z. Wang,[1,56] Z. L. Wang,[70] Z. Y. Wang,[1,61] Ziyi Wang,[61] D. Wei,[68] D. H. Wei,[15] F. Weidner,[66] S. P. Wen,[1] C. W. Wenzel,[4] U. Wiedner,[4] G. Wilkinson,[67] M. Wolke,[73] L. Wollenberg,[4] C. Wu,[38] J. F. Wu,[1,61] L. H. Wu,[1] L. J. Wu,[1,61] X. Wu,[12,f] X. H. Wu,[33] Y. Wu,[69] Y. J. Wu,[30] Z. Wu,[1,56] L. Xia,[69,56] X. M. Xian,[38] T. Xiang,[45,g] D. Xiao,[37,j,k] G. Y. Xiao,[41] H. Xiao,[12,f] S. Y. Xiao,[1] Y. L. Xiao,[12,f] Z. J. Xiao,[40] C. Xie,[41] X. H. Xie,[45,g] Y. Xie,[48] Y. G. Xie,[1,56] Y. H. Xie,[6] Z. P. Xie,[69,56] T. Y. Xing,[1,61] C. F. Xu,[1,61] C. J. Xu,[57] G. F. Xu,[1] H. Y. Xu,[64] Q. J. Xu,[17] W. L. Xu,[64] X. P. Xu,[53] Y. C. Xu,[76] Z. P. Xu,[41] F. Yan,[12,f] L. Yan,[12,f] W. B. Yan,[69,56] W. C. Yan,[79] X. Q. Yan,[1] H. J. Yang,[49,e] H. L. Yang,[33] H. X. Yang,[1] Tao Yang,[1] Y. Yang,[12,f] Y. F. Yang,[42] Y. X. Yang,[1,61] Yifan Yang,[1,61] Z. W. Yang,[37,j,k] M. Ye,[1,56] M. H. Ye,[8] J. H. Yin,[1] Z. Y. You,[57] B. X. Yu,[1,56,61] C. X. Yu,[42] G. Yu,[1,61] T. Yu,[70] X. D. Yu,[45,g] C. Z. Yuan,[1,61] L. Yuan,[2] S. C. Yuan,[1] X. Q. Yuan,[1] Y. Yuan,[1,61] Z. Y. Yuan,[57] C. X. Yue,[38] A. A. Zafar,[71] F. R. Zeng,[48] X. Zeng,[12,f] Y. Zeng,[25,h] Y. J. Zeng,[1,61] X. Y. Zhai,[33] Y. H. Zhan,[57] A. Q. Zhang,[1,61] B. L. Zhang,[1,61] B. X. Zhang,[1] D. H. Zhang,[42] G. Y. Zhang,[20] H. Zhang,[69] H. H. Zhang,[33] H. H. Zhang,[57] H. Q. Zhang,[1,56,61] H. Y. Zhang,[1,56] J. J. Zhang,[50] J. L. Zhang,[75] J. Q. Zhang,[40] J. W. Zhang,[1,56,61] J. X. Zhang,[37,j,k] J. Y. Zhang,[1] J. Z. Zhang,[1,61] Jiawei Zhang,[1,61] L. M. Zhang,[59] L. Q. Zhang,[57] Lei Zhang,[41] P. Zhang,[1] Q. Y. Zhang,[38,79] Shuihan Zhang,[1,61] Shulei Zhang,[25,h] X. D. Zhang,[44] X. M. Zhang,[1] X. Y. Zhang,[53] X. Y. Zhang,[48] Y. Zhang,[67] Y. T. Zhang,[79] Y. H. Zhang,[1,56] Yan Zhang,[69,56] Yao Zhang,[1] Z. H. Zhang,[1] Z. L. Zhang,[33] Z. Y. Zhang,[42] Z. Y. Zhang,[74] G. Zhao,[1] J. Zhao,[38] J. Y. Zhao,[1,61] J. Z. Zhao,[1,56] Lei Zhao,[69,56] Ling Zhao,[1] M. G. Zhao,[42] S. J. Zhao,[79] Y. B. Zhao,[1,56] Y. X. Zhao,[30,61] Z. G. Zhao,[69,56] A. Zhemchugov,[35,a] B. Zheng,[70] J. P. Zheng,[1,56] W. J. Zheng,[1,61] Y. H. Zheng,[61] B. Zhong,[40] X. Zhong,[57] H. Zhou,[48] L. P. Zhou,[1,61] X. Zhou,[74] X. K. Zhou,[6] X. R. Zhou,[69,56] X. Y. Zhou,[38] Y. Z. Zhou,[12,f] J. Zhu,[42] K. Zhu,[1] K. J. Zhu,[1,56,61] L. Zhu,[33] L. X. Zhu,[61] S. H. Zhu,[68] S. Q. Zhu,[41] T. J. Zhu,[12,f] W. J. Zhu,[12,f] Y. C. Zhu,[69,56] Z. A. Zhu,[1,61] J. H. Zou,[1] and J. Zu[69,56]

(BESIII Collaboration)

[1]*Institute of High Energy Physics, Beijing 100049, People's Republic of China*
[2]*Beihang University, Beijing 100191, People's Republic of China*
[3]*Beijing Institute of Petrochemical Technology, Beijing 102617, People's Republic of China*
[4]*Bochum Ruhr-University, D-44780 Bochum, Germany*
[5]*Carnegie Mellon University, Pittsburgh, Pennsylvania 15213, USA*
[6]*Central China Normal University, Wuhan 430079, People's Republic of China*
[7]*Central South University, Changsha 410083, People's Republic of China*
[8]*China Center of Advanced Science and Technology, Beijing 100190, People's Republic of China*
[9]*China University of Geosciences, Wuhan 430074, People's Republic of China*
[10]*Chung-Ang University, Seoul 06974, Republic of Korea*
[11]*COMSATS University Islamabad,*
Lahore Campus, Defence Road, Off Raiwind Road, 54000 Lahore, Pakistan
[12]*Fudan University, Shanghai 200433, People's Republic of China*
[13]*G.I. Budker Institute of Nuclear Physics SB RAS (BINP), Novosibirsk 630090, Russia*
[14]*GSI Helmholtzcentre for Heavy Ion Research GmbH, D-64291 Darmstadt, Germany*
[15]*Guangxi Normal University, Guilin 541004, People's Republic of China*
[16]*Guangxi University, Nanning 530004, People's Republic of China*
[17]*Hangzhou Normal University, Hangzhou 310036, People's Republic of China*
[18]*Hebei University, Baoding 071002, People's Republic of China*
[19]*Helmholtz Institute Mainz, Staudinger Weg 18, D-55099 Mainz, Germany*
[20]*Henan Normal University, Xinxiang 453007, People's Republic of China*
[21]*Henan University of Science and Technology, Luoyang 471003, People's Republic of China*
[22]*Henan University of Technology, Zhengzhou 450001, People's Republic of China*
[23]*Huangshan College, Huangshan 245000, People's Republic of China*
[24]*Hunan Normal University, Changsha 410081, People's Republic of China*
[25]*Hunan University, Changsha 410082, People's Republic of China*
[26]*Indian Institute of Technology Madras, Chennai 600036, India*
[27]*Indiana University, Bloomington, Indiana 47405, USA*
[28a]*INFN Laboratori Nazionali di Frascati, I-00044 Frascati, Italy*
[28b]*INFN Sezione di Perugia, I-06100 Perugia, Italy*
[28c]*University of Perugia, I-06100 Perugia, Italy*
[29a]*INFN Sezione di Ferrara, I-44122 Ferrara, Italy*

[29b]*University of Ferrara, I-44122 Ferrara, Italy*
[30]*Institute of Modern Physics, Lanzhou 730000, People's Republic of China*
[31]*Institute of Physics and Technology, Peace Avenue 54B, Ulaanbaatar 13330, Mongolia*
[32]*Instituto de Alta Investigación, Universidad de Tarapacá,*
Casilla 7D, 1000000 Arica, Chile
[33]*Jilin University, Changchun 130012, People's Republic of China*
[34]*Johannes Gutenberg University of Mainz,*
Johann-Joachim-Becher-Weg 45, D-55099 Mainz, Germany
[35]*Joint Institute for Nuclear Research, 141980 Dubna, Moscow Region, Russia*
[36]*Justus-Liebig-Universitaet Giessen,*
II. Physikalisches Institut, Heinrich-Buff-Ring 16, D-35392 Giessen, Germany
[37]*Lanzhou University, Lanzhou 730000, People's Republic of China*
[38]*Liaoning Normal University, Dalian 116029, People's Republic of China*
[39]*Liaoning University, Shenyang 110036, People's Republic of China*
[40]*Nanjing Normal University, Nanjing 210023, People's Republic of China*
[41]*Nanjing University, Nanjing 210093, People's Republic of China*
[42]*Nankai University, Tianjin 300071, People's Republic of China*
[43]*National Centre for Nuclear Research, Warsaw 02-093, Poland*
[44]*North China Electric Power University, Beijing 102206, People's Republic of China*
[45]*Peking University, Beijing 100871, People's Republic of China*
[46]*Qufu Normal University, Qufu 273165, People's Republic of China*
[47]*Shandong Normal University, Jinan 250014, People's Republic of China*
[48]*Shandong University, Jinan 250100, People's Republic of China*
[49]*Shanghai Jiao Tong University, Shanghai 200240, People's Republic of China*
[50]*Shanxi Normal University, Linfen 041004, People's Republic of China*
[51]*Shanxi University, Taiyuan 030006, People's Republic of China*
[52]*Sichuan University, Chengdu 610064, People's Republic of China*
[53]*Soochow University, Suzhou 215006, People's Republic of China*
[54]*South China Normal University, Guangzhou 510006, People's Republic of China*
[55]*Southeast University, Nanjing 211100, People's Republic of China*
[56]*State Key Laboratory of Particle Detection and Electronics,*
Beijing 100049, Hefei 230026, People's Republic of China
[57]*Sun Yat-Sen University, Guangzhou 510275, People's Republic of China*
[58]*Suranaree University of Technology,*
University Avenue 111, Nakhon Ratchasima 30000, Thailand
[59]*Tsinghua University, Beijing 100084, People's Republic of China*
[60a]*Turkish Accelerator Center Particle Factory Group, Istinye University,*
34010 Istanbul, Turkey
[60b]*Near East University, Nicosia, North Cyprus, 99138, Mersin 10, Turkey*
[61]*University of Chinese Academy of Sciences, Beijing 100049, People's Republic of China*
[62]*University of Groningen, NL-9747 AA Groningen, The Netherlands*
[63]*University of Hawaii, Honolulu, Hawaii 96822, USA*
[64]*University of Jinan, Jinan 250022, People's Republic of China*
[65]*University of Manchester, Oxford Road, Manchester M13 9PL, United Kingdom*
[66]*University of Muenster, Wilhelm-Klemm-Strasse 9, 48149 Muenster, Germany*
[67]*University of Oxford, Keble Road, Oxford OX13RH, United Kingdom*
[68]*University of Science and Technology Liaoning,*
Anshan 114051, People's Republic of China
[69]*University of Science and Technology of China,*
Hefei 230026, People's Republic of China
[70]*University of South China, Hengyang 421001, People's Republic of China*
[71]*University of the Punjab, Lahore-54590, Pakistan*
[72a]*University of Turin, I-10125 Turin, Italy*
[72b]*University of Eastern Piedmont, I-15121 Alessandria, Italy*
[72c]*INFN, I-10125 Turin, Italy*
[73]*Uppsala University, Box 516, SE-75120 Uppsala, Sweden*
[74]*Wuhan University, Wuhan 430072, People's Republic of China*
[75]*Xinyang Normal University, Xinyang 464000, People's Republic of China*
[76]*Yantai University, Yantai 264005, People's Republic of China*
[77]*Yunnan University, Kunming 650500, People's Republic of China*

[78]*Zhejiang University, Hangzhou 310027, People's Republic of China*
[79]*Zhengzhou University, Zhengzhou 450001, People's Republic of China*

(Received 27 February 2023; revised 29 March 2023; accepted 8 May 2023; published 22 May 2023)

Using $(10\,087 \pm 44) \times 10^6$ J/ψ events collected with the BESIII detector, the radiative hyperon decay $\Sigma^+ \to p\gamma$ is studied at an electron-positron collider experiment for the first time. The absolute branching fraction is measured to be $(0.996 \pm 0.021_{\mathrm{stat}} \pm 0.018_{\mathrm{syst}}) \times 10^{-3}$, which is lower than its world average value by 4.2 standard deviations. Its decay asymmetry parameter is determined to be $-0.652 \pm 0.056_{\mathrm{stat}} \pm 0.020_{\mathrm{syst}}$. The branching fraction and decay asymmetry parameter are the most precise to date, and the accuracies are improved by 78% and 34%, respectively.

DOI: 10.1103/PhysRevLett.130.211901

Radiative hyperon decays provide valuable insight into the nature of nonleptonic weak interactions [1]. In general, the radiative decays of a spin-$\frac{1}{2}$ hyperon are described by a parity conserving (P wave) and a parity violating (S wave) amplitude. The nonvanishing parity violating amplitude produces an asymmetric angular distribution of the daughter baryon in the hyperon rest frame, as $dN/d\Omega = (N/4\pi)(1 + \alpha_\gamma \boldsymbol{P}_i \cdot \hat{p})$. Here, $\boldsymbol{P}_i$ is the polarization of the decaying hyperon, $\hat{p}$ is the unit vector of the daughter baryon's momenta in the hyperon rest frame, and α_γ is the decay asymmetry parameter characterizing the mixing of S and P waves. In the limit of unitary symmetry, the parity violating amplitude of radiative hyperon decays is predicted to be small, resulting in $\alpha_\gamma = 0$ [2]. However, the α_γ values measured in experiments are large [3–5]. Of all radiative hyperon decays, the $\Sigma^+ \to p\gamma$ decay was observed first and stimulated continued controversy over several decades. It was first observed in bubble chamber experiments [6], and was studied later at modern particle physics spectrometers [3,7]. The current world average value [8] is dominated by precise measurements using a polarized charged hyperon beam at Fermilab [5,9], where both branching fraction (BF) and α_γ are obtained as ratios to those of the $\Sigma^+ \to p\pi^0$ decay.

Various phenomenological models have been proposed to explain the experimental results of radiative hyperon decays [10–13], but none of them gives a unified picture in describing all radiative hyperon decays. The theoretical predictions given by Ref. [14] in the framework of chiral perturbation theory (ChPT) are consistent with the experimental results of almost all radiative hyperon decays except for $\Sigma^+ \to p\gamma$. Therefore, more precise measurements on $\Sigma^+ \to p\gamma$ are crucial to test theoretical approaches such as ChPT. In addition, it has long been argued that $\Sigma^+ \to pl^+l^- (l = e, \mu)$ decays are good probes for physics beyond the standard model (SM) [15–17]. More precise BF and α_γ measurements of $\Sigma^+ \to p\gamma$ offer critical information on the form factor of $\Sigma^+ \to pl^+l^-$ [17], and thus provide better constraints on the SM predictions for these decays.

The unique properties of $J/\psi \to \Sigma^+\bar{\Sigma}^-$ events produced in electron-positron collisions, e.g., the spin correlation and transverse polarization of hyperon and antihyperon [18,19], and the well defined kinematics, provide ideal conditions to study the decay $\Sigma^+ \to p\gamma$. A double-tagged technique is applied to determine the absolute BF [20]. This approach was applied in a recent work on the $\Lambda \to n\gamma$ decay investigated in the $J/\psi \to \Lambda\bar{\Lambda}$ process by BESIII [21], which achieved a better precision than fixed target experiments. Moreover, the decay $\Sigma^+ \to p\gamma$ and the corresponding charge conjugate one provide a good opportunity to search for CP violation [22], whose experimental information is absent for $\Sigma^+ \to p\gamma$ [23] currently.

In this Letter, using $J/\psi \to \Sigma^+\bar{\Sigma}^-$ decays from $(10\,087 \pm 44) \times 10^6$ J/ψ events [24] collected at BESIII, we report the measurements of the absolute BF and decay asymmetry parameter of $\Sigma^+ \to p\gamma$, as well as a test of CP violation in hyperon decays. Throughout this Letter, charge conjugation is always implied unless noted otherwise.

A detailed description of the design and performance of the BESIII detector can be found in Ref. [25], while the simulation and analysis software framework for BESIII are described in Ref. [26]. First, events of $J/\psi \to \Sigma^+\bar{\Sigma}^-$ are selected with a single-tag (ST) approach, i.e., reconstructing a $\bar{\Sigma}^-$ candidate in one of its dominant decay modes $\bar{\Sigma}^- \to \bar{p}\pi^0$ (BF $= (51.57 \pm 0.30)\%$) [8]. Then, the double-tag (DT) decay $\Sigma^+ \to p\gamma$ is searched for in the system recoiling against the ST $\bar{\Sigma}^-$ hyperon. The corresponding absolute BF is calculated by

$$\mathrm{BF}(\Sigma^+ \to p\gamma) = \frac{N_{\mathrm{DT}}^{\mathrm{obs}} \varepsilon_{\mathrm{ST}}}{N_{\mathrm{ST}}^{\mathrm{obs}} \varepsilon_{\mathrm{DT}}}, \tag{1}$$

where $N_{\mathrm{ST(DT)}}^{\mathrm{obs}}$ and $\varepsilon_{\mathrm{ST(DT)}}$ are the ST (DT) yields and the corresponding detection efficiencies, respectively.

The helicity decay amplitudes of the processes [27], which will be used for the measurement of α_γ, are functions of the five observables $\xi = (\theta_{\Sigma^+}, \theta_p, \phi_p, \theta_{\bar{p}}, \phi_{\bar{p}})$. Here, θ_{Σ^+} is the angle between the Σ^+ hyperon and the electron beam in the J/ψ rest frame, θ_p ($\theta_{\bar{p}}$) and ϕ_p ($\phi_{\bar{p}}$) are the polar and azimuthal angles of the proton (antiproton) with respect to the Σ^+ helicity frame, respectively. The differential cross section is given as $\mathrm{d}\sigma \propto \mathcal{W}(\xi)\mathrm{d}\xi$ with

$$\begin{aligned}\mathcal{W}(\xi) = {} & \mathcal{F}_0(\xi) + \alpha_\psi \mathcal{F}_5(\xi) + \alpha_\gamma \bar{\alpha}_0 \\ & \times \left[\mathcal{F}_1(\xi) + \sqrt{1-\alpha_\psi^2}\cos(\Delta\Phi)\mathcal{F}_2(\xi) + \alpha_\psi \mathcal{F}_6(\xi)\right] \\ & + \sqrt{1-\alpha_\psi^2}\sin(\Delta\Phi)[\alpha_\gamma \mathcal{F}_3(\xi) + \bar{\alpha}_0 \mathcal{F}_4(\xi)], \end{aligned} \tag{2}$$

where α_ψ and $\Delta\Phi$ are the hyperon production parameters of the process $J/\psi \to \Sigma^+\bar{\Sigma}^-$, $\bar{\alpha}_0$ is the decay asymmetry parameter for the $\bar{\Sigma}^- \to \bar{p}\pi^0$ decays, and $\mathcal{F}_i(\xi)$ $(i = 0, 1, \ldots, 6)$ are the angular functions as described in detail in Ref. [27]. The parameters used here are fixed to the values in Ref. [19], except for α_γ to be determined in this analysis.

A sample of Monte Carlo (MC) simulated events of generic J/ψ decays corresponding to the luminosity of data is used to study possible background reactions. On the ST side, the signal MC sample of $J/\psi \to \Sigma^+(\to \text{anything})\bar{\Sigma}^-(\to \bar{p}\pi^0)$ is generated with its helicity decay amplitude. A phase space (PHSP) MC sample of $J/\psi \to \Delta(1232)^+(\to \text{anything})\bar{\Delta}(1232)^-(\to \bar{p}\pi^0)$ is generated to study ST background. On the DT side, MC samples for the $J/\psi \to \Sigma^+(\to p\gamma)\bar{\Sigma}^-(\to \bar{p}\pi^0)$ signal and the dominant background $J/\psi \to \Sigma^+(\to p\pi^0)\bar{\Sigma}^-(\to \bar{p}\pi^0)$ are generated according to their helicity decay amplitudes.

Charged tracks and photon candidates are detected in the main drift chamber and electromagnetic calorimeter, respectively. Requirements on the polar angle, distance of closest approach to the interaction point, particle identification probability of charged tracks, the polar angle, energy, electromagnetic calorimeter time and distance to the nearest charged track of photon candidates are applied as in Ref. [19]. The π^0 candidates are reconstructed from pairs of photon candidates with an invariant mass $M_{\gamma\gamma}$ satisfying $116~\mathrm{MeV}/c^2 < M_{\gamma\gamma} < 148~\mathrm{MeV}/c^2$. A kinematic fit constraining their invariant mass to the π^0 mass [8] is performed on these photon pairs, and the updated four-momentum is used in further analysis.

The candidate ST $\bar{\Sigma}^-$ events are required to have at least one $\bar{p}$ and one π^0, and the $\bar{p}\pi^0$ combination is required to have an invariant mass of $|M_{\bar{p}\pi^0} - M_{\bar{\Sigma}^-}| < 13.5~\mathrm{MeV}/c^2$, where $M_{\bar{\Sigma}^-}$ is the nominal $\bar{\Sigma}^-$ mass [8]. If there is more than one combination satisfying this requirement, the one with the minimum $|M_{\bar{p}\pi^0} - M_{\bar{\Sigma}^-}|$ is kept for further analysis. Finally, the ST yield is obtained from the mass distribution recoiling against the reconstructed $\bar{\Sigma}^-$ candidate, which is defined as

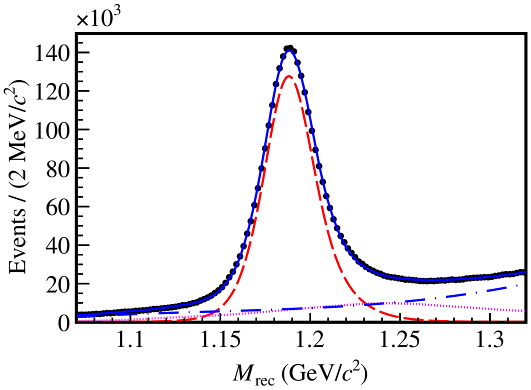

FIG. 1. Fit to the M_{rec} distribution of ST candidates in data. Points with error bars represent data. The blue solid curve is the total fit result. The red dashed curve, magenta dotted curve, and blue dash-dotted curve show the shapes of signal, $J/\psi \to \Delta(1232)^+(\to \text{anything})\bar{\Delta}(1232)^-(\to \bar{p}\pi^0)$ background and other nonpeaking background components, respectively.

$$M_{\mathrm{rec}} = \sqrt{(E_{\mathrm{cms}} - E_{\bar{p}} - E_{\pi^0})^2/c^4 - (\boldsymbol{P}_{\bar{p}} + \boldsymbol{P}_{\pi^0})^2/c^2}. \tag{3}$$

Here, E_{cms} is the center-of-mass energy, $E_{\bar{p}}$ ($\boldsymbol{P}_{\bar{p}}$) and E_{π^0} ($\boldsymbol{P}_{\pi^0}$) are the energies (momenta) of the antiproton and π^0 in the J/ψ rest frame, respectively.

With the above selection criteria, the distribution of M_{rec} of the ST candidates is shown in Fig. 1, where there is a clear peak representing the signal of $J/\psi \to \Sigma^+\bar{\Sigma}^-$. For ST candidates, the background events are dominated by miscombinations and $J/\psi \to \Delta(1232)^+(\to \text{anything})\bar{\Delta}(1232)^-(\to \bar{p}\pi^0)$, which contributes as a broad peak. An unbinned maximum likelihood fit is performed on the M_{rec} distribution to determine the ST yield, with the fit result shown in Fig. 1. In the fit, the signal and $J/\psi \to \Delta(1232)^+(\to \text{anything})\bar{\Delta}(1232)^-(\to \bar{p}\pi^0)$ background are described by their MC simulated shapes convolved with a Gaussian function, which represents the resolution difference between data and MC simulation. Other nonpeaking background is described by a third order polynomial function. The ST yield and the detection efficiency evaluated using the signal MC sample are summarized in Table I.

The signal process $\Sigma^+ \to p\gamma$ is searched for in the remaining charged tracks and photons recoiling against the selected ST $\bar{\Sigma}^-$ candidates. One remaining p and at least one remaining photon candidate are required for DT candidate events. A five-constraint (5C) kinematic fit under the hypothesis $J/\psi \to p\bar{p}\pi^0\gamma$ is performed. The fit constrains the total energy momentum of the final state particles to the four-momentum of J/ψ and the invariant mass of the photon pair on the ST side to the π^0 nominal mass [8]. The χ^2 of the 5C kinematic fit ($\chi^2_{5\mathrm{C}}$) is required to be less than 30. In case of multiple photon candidates on the

TABLE I. The values of $N_{\rm ST}^{\rm obs}$, $\varepsilon_{\rm ST}$, $N_{\rm DT}^{\rm obs}$, and $\varepsilon_{\rm DT}$ for the decays $\Sigma^+ \to p\gamma$ and $\bar{\Sigma}^- \to \bar{p}\gamma$. The BF and α_γ are obtained from both individual and simultaneous fits. The first uncertainties are statistical and the second systematic.

Mode	$\Sigma^+ \to p\gamma$	$\bar{\Sigma}^- \to \bar{p}\gamma$
$N_{\rm ST}^{\rm obs}$	$2\,177\,771 \pm 2285$	$2\,509\,380 \pm 2301$
$\varepsilon_{\rm ST}$ (%)	39.00 ± 0.04	44.31 ± 0.04
$N_{\rm DT}^{\rm obs}$	1189 ± 38	1306 ± 39
$\varepsilon_{\rm DT}$ (%)	21.16 ± 0.03	23.20 ± 0.03
Individual BF (10^{-3})	1.005 ± 0.032	0.993 ± 0.030
Simultaneous BF (10^{-3})	$0.996 \pm 0.021 \pm 0.018$	
Individual α_γ	-0.587 ± 0.082	0.710 ± 0.076
Simultaneous α_γ	$-0.651 \pm 0.056 \pm 0.020$	

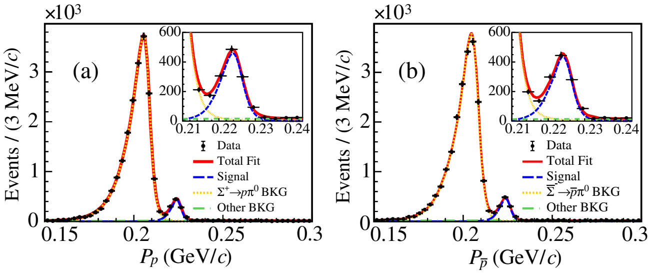

FIG. 2. Fits to the P_p distributions for (a) $\Sigma^+ \to p\gamma$ and (b) $\bar{\Sigma}^- \to \bar{p}\gamma$ candidate events. Points with error bars are data. The red solid curves are the total fit results. The blue dashed, orange dotted, and green dash-dotted curves show the shapes of signal, $\Sigma^+ \to p\pi^0$ background, and other background, respectively. The insets show the details of the fit in the signal region.

DT side, the one with the minimum $\chi^2_{5\rm C}$ is kept. This requirement removes ~68% of the background at the cost of 13.9% of the signal.

MC studies with a generic event type analysis tool [28] indicate that the dominant background events on the DT side are from the processes $J/\psi \to \Sigma^+(\to p\pi^0)\bar{\Sigma}^-(\to \bar{p}\pi^0)$ and $J/\psi \to \Delta(1232)^+(\to p\pi^0)\bar{\Delta}(1232)^-(\to \bar{p}\pi^0)$, denoted as $\Sigma^+ \to p\pi^0$ and $\Delta(1232)^+ \to p\pi^0$ background. To remove the $\Delta(1232)^+ \to p\pi^0$ background, we make use of the lifetime difference between Σ^+ and $\Delta(1232)^+$. A secondary vertex fit [29] is performed for the p and $\bar{p}$ combination. The length (L) from the intersection point to the interaction point shows significantly different distribution for the $\Delta(1232)^+ \to p\pi^0$ background and the signal, as shown in Sec. 2 of the Supplemental Material [30]. The L/σ_L value of the $\Delta(1232)^+ \to p\pi^0$ background is generally less than 1.5, where σ_L is the decay length resolution. By vetoing these events, the $\Delta(1232)^+ \to p\pi^0$ background is reduced by 93% while 78% of the signal is preserved. The remaining $\Sigma^+ \to p\pi^0$ background usually includes a high energy photon from an asymmetric π^0 decay. To suppress this background, a 5C kinematic fit under the $J/\psi \to p\bar{p}\pi^0\gamma\gamma$ hypothesis is performed for all photon pair combinations. A candidate is eliminated if any χ^2 of the kinematic fit under the $J/\psi \to p\bar{p}\pi^0\gamma\gamma$ hypothesis is less than χ^2_{5C} under the signal hypothesis.

After applying all the above selection criteria, the distribution of the proton momentum in the rest frame of Σ^+ (P_p) is shown in Fig. 2. The prominent peak at 0.204 GeV/c is the major background from $\Sigma^+ \to p\pi^0$, and the peaking structure around 0.223 GeV/c is from the $\Sigma^+ \to p\gamma$ signal. The contribution from the $\Delta(1232)^+ \to p\pi^0$ background is negligible.

To obtain the DT signal yield, an unbinned maximum likelihood fit is performed on the P_p distribution. In the fit, the $\Sigma^+ \to p\gamma$ signal and the $\Sigma^+ \to p\pi^0$ background are described by MC simulated shapes convolved with a Gaussian function. A second order polynomial function is included to represent the residual background such as $\Delta(1232)^+ \to p\pi^0$. The fit results are shown in Fig. 2, and the DT signal yields are summarized in Table I. In the fit, the yields of the $\Sigma^+ \to p\pi^0$ and $\bar{\Sigma}^- \to \bar{p}\pi^0$ background are $18\,227.7 \pm 135.0$ and $20\,334.9 \pm 142.6$, respectively. To account for the small difference in the selection efficiencies of charged tracks and photons between data and MC simulation, an efficiency correction has been performed on the DT side [19]. The resultant DT efficiencies and the BFs are also summarized in Table I. The BFs for $\Sigma^+ \to p\gamma$ and $\bar{\Sigma}^- \to \bar{p}\gamma$ are consistent with each other within their uncertainties. Therefore, a simultaneous fit assuming the same BF between the charge conjugate channels is performed. The resultant BF is also shown in Table I.

The decay asymmetry parameter α_γ is determined by an angular analysis according to Eq. (2). To further improve the purity of the data sample used for the α_γ measurements, two additional kinematic fits under the hypotheses of $J/\psi \to p\bar{p}\pi^0 + \pi^0$ and $J/\psi \to p\bar{p}\pi^0 + \gamma$ are performed for the surviving DT candidates, where the momenta information of the π^0 and photon are missing in the fit. The DT candidates are removed if $\chi^2_{p\bar{p}\pi^0+\pi^0} < \chi^2_{p\bar{p}\pi^0+\gamma}$, where $\chi^2_{p\bar{p}\pi^0+\pi^0}$ and $\chi^2_{p\bar{p}\pi^0+\gamma}$ are the χ^2 from the two kinematic fits. Finally, 2345 events (including 243 background events) for the two charge conjugate modes in the signal region $0.215\ {\rm GeV}/c < P_p < 0.235\ {\rm GeV}/c$ are used in the following analysis.

α_γ is obtained from an unbinned maximum likelihood fit with the likelihood function defined as

$$\mathcal{L}(H) = \prod_{i=1}^{N} \frac{\mathcal{W}(\xi_i, H)\varepsilon(\xi_i)}{C(H)}, \qquad (4)$$

where $H = (\alpha_\psi, \Delta\Phi, \alpha_\gamma, \bar{\alpha}_0)$ represents the decay parameters, N is the total number of DT candidate events, i is the corresponding event index, $\mathcal{W}(\xi_i, H)$ is the square of the decay amplitude as defined in Eq. (2), $\varepsilon(\xi_i)$ is the detection efficiency, and $C(H)$ is the normalization factor calculated with the PHSP MC sample [18]. Because of the small number of events, the parameters α_ψ, $\Delta\Phi$, and $\bar{\alpha}_0$ are fixed to those in Ref. [19] in the fit.

The value of α_γ is obtained by minimizing the likelihood function $S = -(\ln \mathcal{L}_{\text{data}} - \ln \mathcal{L}_{\text{bkg}})$, where $\mathcal{L}_{\text{data}}$ is the likelihood value from the data sample, and $\mathcal{L}_{\text{bkg}}$ represents the background contributions including $\Sigma^+ \to p\pi^0$ and other background components. The former background contribution is estimated with a MC simulated event sample that is 5 times the size of data and is generated according to its decay amplitude. The latter is estimated with data events in the sideband region defined as $0.11\ \text{GeV}/c < P_p < 0.16\ \text{GeV}/c$ and $0.24\ \text{GeV}/c < P_p < 0.29\ \text{GeV}/c$. $\mathcal{L}_{\text{bkg}}$ is estimated with the above samples and normalized to data. The fits are performed for the $\Sigma^+ \to p\gamma$ and $\bar{\Sigma}^- \to \bar{p}\gamma$ decays individually. The α_γ results are consistent within their uncertainties and summarized in Table I. Further, a simultaneous fit, assuming the same magnitude but opposite sign for the decay asymmetry parameters of the charge conjugate channels, is also performed, and the result is also shown in Table I.

To visualize the effect of the decay asymmetry, two moments are calculated for $m = 8$ intervals in $\cos\theta_{\Sigma^+}$:

$$M_1(\cos\theta_{\Sigma^+}) = \frac{m}{N}\sum_{i=1}^{N_k} \cos\theta_{\bar{p}}^i \cos\theta_p^i,$$

$$M_2(\cos\theta_{\Sigma^+}) = \frac{m}{N}\sum_{i=1}^{N_k} \sin\theta_p^i \sin\phi_p^i, \qquad (5)$$

where N is the total number of events and N_k is the number of events in the kth $\cos\theta_{\Sigma^+}$ interval. Figure 3 shows the comparison of moments between data and MC projection based on the fit. Good data-MC consistencies are observed.

The systematic uncertainties due to proton tracking and particle identification (0.4%), as well as photon detection (0.3%), are studied with $J/\psi \to p\bar{p}\pi^+\pi^-$ and $J/\psi \to \gamma\mu^+\mu^-$ control samples. The uncertainties of χ^2 requirements on the kinematic fits (0.9%) and decay length requirement (0.4%) are obtained by applying corresponding requirements on a $J/\psi \to \Sigma^+(\to p\pi^0)\bar{\Sigma}^-(\to \bar{p}\pi^0)$ control sample. The uncertainties of ST (0.4%) and DT (1.2%) yields are estimated by changing the fit parameters. The decay parameters used for signal MC generation are varied by $\pm 1\sigma$ [19] to study the MC model related uncertainty (0.6%). Details can be found in the Supplemental Material [30]. By assuming all the sources to be independent, the total systematic uncertainty in the BF measurement is 1.8% by summing up all above values in quadrature.

The systematic uncertainties in the determination of the decay asymmetry parameter α_γ are separated into two categories: the fit-related uncertainties and event selection uncertainties. The fit-related uncertainties are estimated with alternative fits by shifting the sideband region (0.004), changing the signal region in the fit (0.014), varying the number of background events by $\pm 1\sigma$ (0.002), and varying the fixed decay parameters by $\pm 1\sigma$ [19] (0.011), individually.

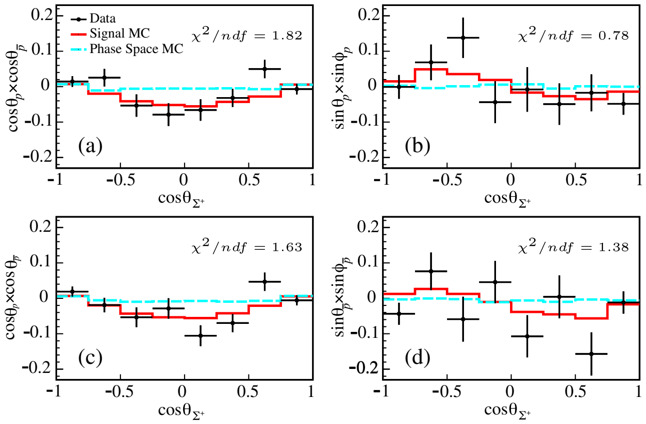

FIG. 3. Moment distributions for (a),(b) $\bar{\Sigma}^- \to \bar{p}\gamma$ and (c), (d) $\Sigma^+ \to p\gamma$. The black points with error bars are data. The cyan dashed curves are the phase space MC simulation. The red solid curves show the MC simulation based on the fit results. For the comparison between charge conjugate channels, plots (c),(d) adopt the polar angle of $\bar{\Sigma}^-$ hyperon as the abscissa variable.

For the event selection induced uncertainties, only the angular dependent event selection criteria are considered, since other effects are negligible. For each requirement, its dependence on the angular distribution and effect on the systematic uncertainty are detailed in the Supplemental Material [30]. The systematic uncertainty due to the track detection efficiency (0.001) is estimated by performing an efficiency correction on the PHSP MC. The decay length requirement (0.005) and $\chi^2_\gamma < \chi^2_{\pi^0}$ requirement (0.006) uncertainties are studied with a $J/\psi \to \Sigma^+(\to p\pi^0)\bar{\Sigma}^-(\to \bar{p}\pi^0)$ control sample. The total systematic uncertainty is assigned to be 0.020 by adding all individual uncertainties quadratically.

Based on the above results, the CP asymmetry is calculated using the BFs and decay asymmetry parameters between the charge conjugate channels:

$$\Delta_{CP} = \frac{\mathcal{B}_+ - \mathcal{B}_-}{\mathcal{B}_+ + \mathcal{B}_-} = 0.006 \pm 0.011_{\text{stat}} \pm 0.004_{\text{syst}},$$

$$A_{CP} = \frac{\alpha_- + \alpha_+}{\alpha_- - \alpha_+} = 0.095 \pm 0.087_{\text{stat}} \pm 0.018_{\text{syst}}.$$

Here, $\mathcal{B}_+$ (α_+) denotes the BF (α_γ) of $\Sigma^+ \to p\gamma$ and $\mathcal{B}_-$ (α_-) is that of $\bar{\Sigma}^- \to \bar{p}\gamma$. The systematic uncertainties of Δ_{CP} and A_{CP} only consider the uncorrelated uncertainties of $B_{+/-}$ and $\alpha_{+/-}$. This represents the first search for CP

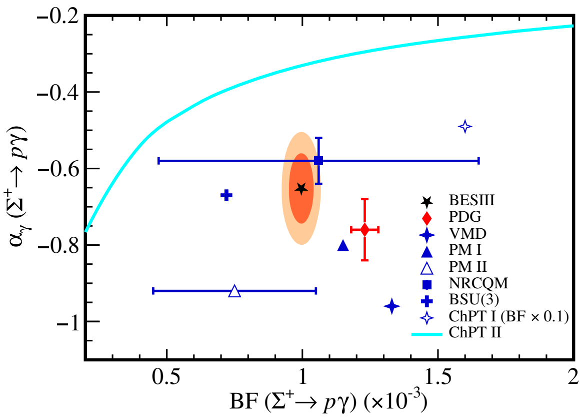

FIG. 4. Distribution of α_γ versus BF of the $\Sigma^+ \to p\gamma$ decay. The black star denotes the results measured by this work and the orange contours correspond to the 68%/95% confidence level of the results. The red diamond represents the PDG values [8] of the BF and α_γ. The cyan colored line shows the predicted α_γ as a function of BF cited from Ref. [14]. Other symbols in blue stand for the results predicted by the vector meson dominance model (VMD) [31], pole model (PM I refers to Ref. [10] and PM II refers to Ref. [11]), nonrelativistic constituent quark model (NRCQM) [12], broken SU(3) model [BSU(3)] [32] and another ChPT model [33].

violation in $\Sigma^+ \to p\gamma$. No obvious *CP* violation is observed.

In summary, using $(10\,087 \pm 44) \times 10^6$ J/ψ events collected with the BESIII detector, the radiative hyperon decay $\Sigma^+ \to p\gamma$ is studied at an electron-positron collider for the first time. The absolute BF of this decay is determined to be $(0.996 \pm 0.021_{\rm stat} \pm 0.018_{\rm syst}) \times 10^{-3}$, with a decay asymmetry parameter of $-0.651 \pm 0.056_{\rm stat} \pm 0.020_{\rm syst}$. Two independent observables between the two charge conjugate channels, A_{CP} and Δ_{CP}, are used to search for *CP* violation, and no evidence of *CP* violation is found. The accuracies of the BF and α_γ are improved by 78% and 34%, respectively. The comparison between the measurement results with the Particle Data Group (PDG) values and theoretical predictions are shown in Fig. 4. The measured BF is lower than the PDG value [8] by 4.2σ, where all previous measurement results were obtained as relative ratios to $\Sigma^+ \to p\pi^0$. The decay asymmetry parameter is consistent with the world average value within 1.1σ. A similar BF difference is also observed in another radiative hyperon decay $\Lambda \to n\gamma$ [21] at BESIII. With the updated BF and α_γ results of $\Sigma^+ \to p\gamma$, further theoretical efforts are needed to clarify the physics of radiative hyperon decays. The SM prediction of $\Sigma^+ \to pl^+l^-$ decays can also be further improved [17] to search for new physics beyond the SM.

The authors thank Professor L. S. Geng and Professor X. G. He for helpful discussion. The BESIII Collaboration thanks the staff of BEPCII and the IHEP computing center and the supercomputing center of USTC for their strong support. This work is supported in part by National Key R&D Program of China under Contracts No. 2020YFA0406300, No. 2020YFA0406400; National Natural Science Foundation of China (NSFC) under Contracts No. 11335008, No. 11625523, No. 11635010, No. 11705192, No. 11735014, No. 11835012, No. 11935015, No. 11935016, No. 11935018, No. 11950410506, No. 11961141012, No. 12022510, No. 12025502, No. 12035009, No. 12035013, No. 12061131003, No. 12105276, No. 12122509, No. 12192260, No. 12192261, No. 12192262, No. 12192263, No. 12192264, No. 12192265; the Chinese Academy of Sciences (CAS) Large-Scale Scientific Facility Program; the CAS Center for Excellence in Particle Physics (CCEPP); Joint Large-Scale Scientific Facility Funds of the NSFC and CAS under Contracts No. U1732263, No. U1832103, No. U1832207, No. U2032111; CAS Key Research Program of Frontier Sciences under Contracts No. QYZDJ-SSW-SLH003, No. QYZDJ-SSW-SLH040; 100 Talents Program of CAS; The Institute of Nuclear and Particle Physics (INPAC) and Shanghai Key Laboratory for Particle Physics and Cosmology; The Double First-Class university project foundation of USTC; ERC under Contract No. 758462; European Union's Horizon 2020 research and innovation programme under Marie Sklodowska-Curie grant agreement under Contract No. 894790; German Research Foundation DFG under Contracts No. 443159800, No. 455635585, Collaborative Research Center CRC 1044, FOR5327, GRK 2149; Istituto Nazionale di Fisica Nucleare, Italy; Ministry of Development of Turkey under Contract No. DPT2006K-120470; National Research Foundation of Korea under Contract No. NRF-2022R1A2C1092335; National Science and Technology fund; National Science Research and Innovation Fund (NSRF) via the Program Management Unit for Human Resources & Institutional Development, Research and Innovation under Contract No. B16F640076; Polish National Science Centre under Contract No. 2019/35/O/ST2/02907; Suranaree University of Technology (SUT), Thailand Science Research and Innovation (TSRI), and National Science Research and Innovation Fund (NSRF) under Contract No. 160355; The Royal Society, UK under Contract No. DH160214; The Swedish Research Council; U.S. Department of Energy under Contract No. DE-FG02-05ER41374.

---

[a] Also at the Moscow Institute of Physics and Technology, Moscow 141700, Russia.

[b] Also at the Novosibirsk State University, Novosibirsk 630090, Russia.

[c] Also at the NRC "Kurchatov Institute", PNPI, 188300 Gatchina, Russia.

[d]Also at Goethe University Frankfurt, 60323 Frankfurt am Main, Germany.

[e]Also at Key Laboratory for Particle Physics, Astrophysics and Cosmology, Ministry of Education; Shanghai Key Laboratory for Particle Physics and Cosmology; Institute of Nuclear and Particle Physics, Shanghai 200240, People's Republic of China.

[f]Also at Key Laboratory of Nuclear Physics and Ion-beam Application (MOE) and Institute of Modern Physics, Fudan University, Shanghai 200443, People's Republic of China.

[g]Also at State Key Laboratory of Nuclear Physics and Technology, Peking University, Beijing 100871, People's Republic of China.

[h]Also at School of Physics and Electronics, Hunan University, Changsha 410082, China.

[i]Also at Guangdong Provincial Key Laboratory of Nuclear Science, Institute of Quantum Matter, South China Normal University, Guangzhou 510006, China.

[j]Also at Frontiers Science Center for Rare Isotopes, Lanzhou University, Lanzhou 730000, People's Republic of China.

[k]Also at Lanzhou Center for Theoretical Physics, Lanzhou University, Lanzhou 730000, People's Republic of China.

[l]Also at the Department of Mathematical Sciences, IBA, Karachi, Pakistan.

[1] R. E. Behrends, Phys. Rev. **111**, 1691 (1958).

[2] Y. Hara, Phys. Rev. Lett. **12**, 378 (1964).

[3] M. Kobayashi, J. Haba, T. Homma, H. Kawai, K. Miyake, T. S. Nakamura, N. Sasao, and Y. Sugimoto, Phys. Rev. Lett. **59**, 868 (1987).

[4] S. Teige *et al.*, Phys. Rev. Lett. **63**, 2717 (1989); C. James, K. Heller, P. Border, J. Dworkin, O. E. Overseth *et al.*, Phys. Rev. Lett. **64**, 843 (1990); T. Dubbs, I. F. Albuquerque, N. F. Bondar, R. Carrigan, Jr., D. Chen *et al.*, Phys. Rev. Lett. **72**, 808 (1994); A. Alavi-Harati *et al.* (KTeV Collaboration), Phys. Rev. Lett. **86**, 3239 (2001).

[5] M. Foucher, I. F. Albuquerque, N. F. Bondar, R. Carrigan, Jr., D. Chen *et al.* (E761 Collaboration), Phys. Rev. Lett. **68**, 3004 (1992).

[6] M. Bazin, H. Blumenfeld, U. Nauenberg, L. Seidlitz, and C. Y. Chang, Phys. Rev. Lett. **14**, 154 (1965); L. K. Gershwin, M. Alston-Garnjost, R. O. Bangerter, A. Barbaro-Galtieri, T. S. Mast, F. T. Solmitz, and R. D. Tripp, Phys. Rev. **188**, 2077 (1969); A. Manz, S. Reucroft, R. Settles, G. Wolf, J. Marraffino, C. Roos, J. Waters, and M. Webster, Phys. Lett. B **96**, 217 (1980); G. Ang *et al.*, Z. Phys. **228**, 151 (1969).

[7] N. P. Hessey *et al.*, Z. Phys. C **42**, 175 (1989); S. F. Biagi *et al.* (Bristol-Geneva-Heidelberg-Lausanne-Queen Mary Coll-Rutherford), Z. Phys. C **28**, 495 (1985).

[8] R. L. Workman *et al.* (Particle Data Group), Prog. Theor. Exp. Phys. **2022**, 083C01 (2022).

[9] S. Timm, I. F. Albuquerque, N. F. Bondar, R. Carrigan, Jr., D. Chen *et al.* (E761 Collaboration), Phys. Rev. D **51**, 4638 (1995).

[10] M. B. Gavela, A. L. Yaouanc, L. Oliver, O. Pène, J. C. Raynal, and T. N. Pham, Phys. Lett. **101B**, 417 (1981).

[11] G. Nardulli, Phys. Lett. B **190**, 187 (1987).

[12] P. Y. Niu, J. M. Richard, Q. Wang, and Q. Zhao, Chin. Phys. C **45**, 013101 (2020).

[13] I. I. Balitsky, V. M. Braun, and A. V. Kolesnichenko, Nucl. Phys. **B312**, 509 (1989); D. Chang, arXiv:hep-ph/0011163; E. N. Dubovik, V. S. Zamiralov, S. N. Lepshokov, and A. E. Shkolnikov, Phys. At. Nucl. **71**, 136 (2008); P. Źenczykowski, Acta Phys. Pol. B **51**, 2111 (2020).

[14] R. X. Shi, S. Y. Li, J. X. Lu, and L. S. Geng, Sci. Bull. **67**, 2298 (2022).

[15] M. Pospelov, Phys. Rev. D **80**, 095002 (2009).

[16] L. S. Geng, J. M. Camalich, and R. X. Shi, J. High Energy Phys. 02 (2022) 178.

[17] X. G. He, J. Tandean, and G. Valencia, J. High Energy Phys. 10 (2018) 040.

[18] M. Ablikim *et al.* (BESIII Collaboration), Nat. Phys. **15**, 631 (2019).

[19] M. Ablikim *et al.* (BESIII Collaboration), Phys. Rev. Lett. **125**, 052004 (2020).

[20] R. M. Baltrusaitis *et al.* (MARK III Collaboration), Phys. Rev. Lett. **56**, 2140 (1986).

[21] M. Ablikim *et al.* (BESIII Collaboration), Phys. Rev. Lett. **129**, 212002 (2022).

[22] J. F. Donoghue, X. G. He, and S. Pakvasa, Phys. Rev. D **34**, 833 (1986); J. Tandean and G. Valencia, Phys. Rev. D **67**, 056001 (2003).

[23] X. Q. Li, Y. S. Li, J. Q. Zhang, P. Y. Zhao, and Q. Zhao, Commun. Theor. Phys. **19**, 475 (1993); X. L. Chen, C. S. Gao, and X. Q. Li, Phys. Rev. D **51**, 2271 (1995).

[24] M. Ablikim *et al.* (BESIII Collaboration), Chin. Phys. C **46**, 074001 (2022).

[25] M. Ablikim *et al.* (BESIII Collaboration), Nucl. Instrum. Methods Phys. Res., Sect. A **614**, 345 (2010); K. X. Huang *et al.*, Nucl. Sci. Tech. **33**, 142 (2022).

[26] W. Li *et al.*, Proc. Int. Conf. Comput. High Energy and Nucl. Phys. 225 (2006); D. M. Asner *et al.*, Int. J. Mod. Phys. A **24S1**, 499 (2009); J. Zhang *et al.*, Radiat. Detect. Technol. Methods **2**, 1 (2018).

[27] G. Fäldt and A. Kupsc, Phys. Lett. B **772**, 16 (2017); E. Perotti, G. Fäldt, A. Kupsc, S. Leupold, and J. J. Song, Phys. Rev. D **99**, 056008 (2019).

[28] X. Y. Zhou, S. X. Du, G. Li, and C. P. Shen, Comput. Phys. Commun. **258**, 107540 (2021).

[29] M. Xu *et al.*, Chin. Phys. C **34**, 92 (2010).

[30] See Supplemental Material at http://link.aps.org/supplemental/10.1103/PhysRevLett.130.211901 for additional details on the study of systematic uncertainties.

[31] P. Żenczykowski, Phys. Rev. D **44**, 1485 (1991).

[32] P. Żenczykowski, Phys. Rev. D **73**, 076005 (2006).

[33] B. Borasoy and B. R. Holstein, Phys. Rev. D **59**, 054019 (1999).